Mapping the Differential Distribution of Proteoglycan Core Proteins in the Adult Human Retina, Choroid, and Sclera

KEENAN, Tiarnan DL, CLARK, Simon J, UNWIN, Richard D, RIDGE, Liam, DAY, Anthony J and BISHOP, Paul N

Published version

KEENAN, Tiarnan DL, CLARK, Simon J, UNWIN, Richard D, RIDGE, Liam, DAY, Anthony J and BISHOP, Paul N (2012). Mapping the Differential Distribution of Proteoglycan Core Proteins in the Adult Human Retina, Choroid, and Sclera. Investigative Opthalmology & Visual Science, 53 (12), 7528-7538.

Mapping the Differential Distribution of Proteoglycan Core Proteins in the Adult Human Retina, Choroid, and Sclera

Tiarnan D. L. Keenan,[1,3,4] *Simon J. Clark,*[1,4] *Richard D. Unwin,*[4] *Liam A. Ridge,*[2] *Anthony J. Day,*[*,2] *and Paul N. Bishop*[*,1,3,4]

Purpose. To examine the presence and distribution of proteoglycan (PG) core proteins in the adult human retina, choroid, and sclera.

Methods. Postmortem human eye tissue was dissected into Bruch's membrane/choroid complex, isolated Bruch's membrane, or neurosensory retina. PGs were extracted and partially purified by anion exchange chromatography. Trypsinized peptides were analyzed by tandem mass spectrometry and PG core proteins identified by database search. The distribution of PGs was examined by immunofluorescence microscopy on human macular tissue sections.

Results. The basement membrane PGs perlecan, agrin, and collagen-XVIII were identified in the human retina, and were present in the internal limiting membrane, blood vessel walls, and Bruch's membrane. The hyalectans versican and aggrecan were also detected. Versican was identified in Bruch's membrane, while aggrecan was distributed throughout the retina, choroid, and sclera. The cartilage link protein HAPLN1 was abundant in the interphotoreceptor matrix and sclera, while HAPLN4 (brain link protein 2) was found throughout the retina and choroid. The small leucine-rich repeat PG (SLRP) family members biglycan, decorin, fibromodulin, lumican, mimecan, opticin, and prolargin were present, with different patterns of distribution in the retina, choroid, and sclera.

Conclusions. A combination of proteomics and immunohistochemistry approaches has provided for the first time a comprehensive analysis of the presence and distribution of PG core proteins throughout the human retina, choroid, and sclera. This complements our knowledge of glycosaminoglycan chain distribution in the human eye, and has important implications for understanding the structure and functional regulation of the eye in health and disease. (*Invest Ophthalmol Vis Sci.* 2012;53:7528–7538) DOI:10.1167/iovs.12-10797

Proteoglycans (PGs) are present in mammalian tissues, both on cell surfaces and in the extracellular matrix, where they play crucial roles in development, homeostasis, and disease.[1,2] PGs are composed of a core protein covalently bound to one or more glycosaminoglycan (GAG) chains, where the core protein typically consists of multiple domains with distinct structural and binding features.[3] PGs may be classified by their associated GAG chain into heparan sulfate (HS), chondroitin sulfate (CS), dermatan sulfate (DS), and keratan sulfate (KS) PGs. However, PGs are also divided into families based on the structural features of their core protein.[4] Important PG classes in the extracellular matrix include the basement membrane PGs, the hyalectans (or lecticans), and the small leucine-rich repeat PG (SLRP) family. Some SLRP family members are part-time PGs, and others such as opticin are always substituted with oligosaccharides instead of GAGs.[2]

PGs interact with many biologically active molecules via their core protein domains, as well as their GAG chains; as such, they are known to play important roles in the interactions between cells and the extracellular matrix, including the regulation of cell differentiation, proliferation, adhesion and migration.[1,2] In the eye, both CS PGs and HS PGs are important in determining axonal guidance from the retina.[5] In addition, CS PGs are essential in maintaining adhesion between RPE cells and the neurosensory retina.[6] In Bruch's membrane, PGs are involved in the regulation of cell-matrix interactions, signaling and inflammation, and contribute to its filtration properties.[7] Importantly, PGs may be implicated in the pathogenesis of AMD, and poor binding of the disease-associated 402H variant of complement factor H to PGs in Bruch's membrane may provide a potential disease mechanism for AMD.[8–10]

Recently, the distribution of PGs in the adult human retina, choroid, and sclera has been examined indirectly through immunolocalization of their associated GAG chains.[11] We found that HS, CS, and DS were present throughout the retina and choroid, but that KS was detected only in the sclera. HS labeling was strong in basement membrane structures and particular retinal layers (e.g., the nerve fiber layer). In addition, a differential distribution of GAG chains was observed depending on sulphation state. For example, unsulfated CS and 6-O-sulfated CS were prominent in the interphotoreceptor

From the [1]Centre for Ophthalmology and Vision Research, Institute of Human Development and the [2]Wellcome Trust Centre for Cell-Matrix Research, Faculty of Life Sciences, University of Manchester, Manchester, United Kingdom; and the [3]Manchester Royal Eye Hospital and [4]Centre for Advanced Discovery and Experimental Therapeutics, Central Manchester University Hospitals NHS Foundation Trust, Manchester Academic Health Science Centre, Manchester, United Kingdom.

Supported by a Fight for Sight Clinical Fellowship (1866; TDLK); the Medical Research Council (G0900592); the NIHR Manchester Biomedical Research Centre; grants from the BBSRC; Wellcome Trust; and the University of Manchester Strategic Fund.

Submitted for publication August 18, 2012; revised October 11, 2012; accepted October 12, 2012.

Disclosure: **T.D.L. Keenan**, None; **S.J. Clark**, None; **R.D. Unwin**, None; **L.A. Ridge**, None; **A.J. Day**, None; **P.N. Bishop**, None

*Each of the following is a corresponding author: Paul N. Bishop, Institute of Human Development, AV Hill Building, University of Manchester, Oxford Road, Manchester M13 9PT; paul.bishop@manchester.ac.uk.

Anthony J. Day, Faculty of Life Sciences, Michael Smith Building, University of Manchester, Oxford Road, Manchester M13 9PT; anthony.day@manchester.ac.uk.

Investigative Ophthalmology & Visual Science, November 2012, Vol. 53, No. 12

matrix (IPM), while the internal limiting membrane (ILM) contained GAG chains with little or no sulfation.

Particular PG core proteins have been studied by immunohistochemistry in mouse, rat and chick retinal tissue,[3,12–15] and in some cases, in human retina.[16–19] However, there has been no comprehensive analysis of the distribution of PG core proteins in the human eye. This should be useful to our understanding of the development and structure of the retina, choroid, and sclera, and may provide important insights into the pathophysiology of these complex tissues. In this study, we have used a proteomics approach to search for PG core proteins in human ocular tissue, and employed immunofluorescence microscopy to compile a map of these PGs in the human retina, choroid, and sclera.

Methods

Tissue Preparation for Proteomic Analysis

Postmortem human eyes were obtained from the Manchester Eye Bank after removal of the corneas for transplantation. In all cases, prior consent had been obtained for the ocular tissue to be used for research, and guidelines established in the Human Tissue Act 2004 were followed. Our research adhered to the tenets of the Declaration of Helsinki. Eyes were from adult human donors without known retinal disease or visual impairment.

Ten globes (five pairs from five donors, aged between 60 and 83 years) were dissected, removing the iris, lens, and vitreous body, to obtain the neurosensory retina and the tissue complex that includes the RPE, Bruch's membrane, and choroid (henceforth known as Bruch's/choroid complex). Ten further globes (five pairs from another five donors, aged between 63 and 75 years) were dissected to obtain isolated Bruch's membrane, by removing the RPE and the choroid through repeated application of a cell scraper until a homogeneous grey tissue layer was left.

The tissues described above were pooled (i.e., each from 10 globes) to produce three samples as follows: Bruch's/choroid complex, Bruch's membrane, and neurosensory retina. These tissue samples were cut up separately into fine pieces. PGs were solubilized from each of the three samples using guanidinium chloride extraction. Briefly, each sample was added to 20 mL 4 M guanidine HCl, 0.5 M NaOAc, and 0.5 mL protease inhibitor cocktail (AEBSF, aprotinin, bestatin, EDTA, E-64, and pepstatin [Sigma, Poole, UK]) at pH 5.8, and left for 18 hours at 4°C on a rotating mixer. Each sample then underwent centrifugation, and the supernatant was dialyzed twice (1:50 volume, for 16 hours at room temperature) against the DEAE starting buffer: 8 M urea, 50 mM Tris HCl at pH 6.8. Samples were filtered with a 0.22-μm filter prior to use. Anion exchange chromatography was performed separately for the three samples using a 1.6 mL DEAE Sepharose Fast Flow column (GE Healthcare Life Sciences, Little Chalfont, UK), equilibrated with 5-column volumes of 50 mM Tris HCl at pH 6.8, followed by a gradient of 0 to 1 M NaCl in 50 mM Tris HCl, pH 6.8, over 13-column volumes; the fractions collected were each of volume 500 μL.

Chromatography fractions were probed with Alcian blue (Sigma) using the critical electrolyte method[20] in order to identify those fractions with highest concentration of PGs. Here, 100 μL of each fraction was applied to a nitrocellulose membrane under vacuum in a slot blot. The membrane was blocked by submersion for 1 hour in 200 mL 1% (w/v) bovine serum albumin in PBS (Oxoid; 137 mM NaCl, 2.6 mM KCl, 8.2 mM Na_2HPO_4, 1.5 mM KH_2PO_4, pH 7.3) at room temperature on a mixing tray. Following this, the membrane was submerged in 200 mL Alcian blue (0.2% [w/v] at pH 2.5 in PBS) for 20 minutes, and destained by submersion in 0.05 M $MgCl_2$, 3% (v/v) acetic acid, with three changes for 10 minutes each. The nitrocellulose membrane was dried and the degree of Alcian blue staining was analyzed using densitometry measurements.

Mass Spectrometric Analysis

Fractions that produced the highest Alcian blue staining were desalted and exchanged into 50 mM ammonium bicarbonate (at pH 7.5) using size exclusion spin columns (10 kDa molecular weight cutoff [MWCO]; GE Healthcare Life Sciences), reducing the volume of each to 100 μL. The fractions were then reduced and alkylated, with addition of dithiothreitol (10 μL at 10 mM for 2 hours at 30°C) and then iodoethamide (10 μL at 20 mM for 20 minutes at room temperature in the dark). Fractions were trypsinized (mass spectrometry grade trypsin (Sigma) at 1.2 μg per 120 μL sample) for 16 hours at 37°C, and trypsinized peptides were separated from GAG chains using size exclusion spin columns (5 kDa MWCO). Tandem mass spectrometry of the trypsinized peptides was performed using a chromatography system (nanoACQUITY UPLC; Waters Corporation, Milford, MA) online to a mass spectrometer (QSTAR Elite Q-TOF; AB SCIEX, Framingham, MA), employing standard methods.[21] The results were analyzed by means of the MASCOT search algorithm against a human UniProt database. For each tissue type, the list of proteins identified was surveyed manually for all PG core proteins.

Preparation of Tissue Sections for Immunofluorescence Microscopy

As above, donor eyes were obtained from the Manchester Eye Bank. Each immunohistochemical experiment reported in this study was performed separately on tissue sections of eyes from three different donors (males aged 46, 47, and 86 years) without known retinal disease or visual impairment.

Donor eyes were fixed within 24 hours post mortem in 4% (v/v) formaldehyde for two hours at room temperature, as described previously.[8,11] Briefly, the macular region was removed using a 5-mm biopsy punch (SCHUCO International, London, UK) and further fixed in 4% (v/v) formaldehyde for 16 hours at 4°C. Each sample was set in OCT cryoprotectant (RA Lamb, Eastbourne, UK); 5-μm tissue slices were made using a cryostat (Leica CM1850; Leica Biosystems, Buffalo Grove, IL) and these were mounted on poly-L-lysine coated microscope slides (Menzel-Gläser, Saarbrückene, Germany). Slides were stored at −80°C prior to use in immunohistochemistry experiments.

Immunohistochemistry for Proteoglycan Core Proteins

Immunohistochemistry experiments were performed by application of particular antibodies specific for PG core proteins, in association with fluorescently labeled secondary antibodies, as summarized in Table 1. Where required, tissue sections underwent enzymatic treatment and/or additional steps before application of the antibody (as described below).

Prior to staining or enzymatic pretreatments, microscope slides were incubated with chilled (−20°C) histological grade acetone (Sigma) for 20 seconds before being thoroughly washed in PBS. Squares were drawn around each tissue section using a hydrophobic barrier pen (VectaLabs, Peterborough, UK) to prevent treatment contamination from adjacent samples. Pretreatment with chondroitin ABC lyase (0.2 U/mL in PBS at 37°C for 2 hours; Sigma) was undertaken where required (see Table 1). In the case of experiments for HAPLN1, pretreatment involved reduction (10 mM dithiothreitol in 50 mM Tris HCl, 200 mM NaCl, pH 7.4 at 37°C for 2 hours) and alkylation (40 mM iodoacetamide in PBS at 37°C for 1 hour) followed by digestion with chondroitin AC lyase (0.25 U/mL in PBS at 37°C for 2 hours; Sigma). The tissue sections were then blocked by incubation at room temperature for 1 hour with PBS containing 1 mg/mL BSA, 1% (v/v) goat serum and 0.1% (v/v) nonionic surfactant (Triton X-100; Sigma).

For each experiment, the relevant antibody was diluted in blocking buffer (see Table 1); applied to tissue sections (100 μL/section); and incubated for 16 hours at 4°C. After extensive washing with PBS, the appropriate Alexa Fluor 488–conjugated secondary antibody (i.e., goat

Table 1. List of Antibodies Used for Labeling Specific Proteoglycan Core Proteins

	Perlecan	Agrin	Collagen-XVIII	Versican		Aggrecan		Brevican	Decorin
Antibody	5C9 mAb	6D2 mAb	6C4 mAb	2B1 mAb	12C5 mAb	179509 mAb	B5 pAb	450616 mAb	115402 mAb
Source	DSHB*	DSHB	DSHB	Gift of T Wight		R&D Systems	Gift of T Hardingham	R&D Systems	R&D Systems
Epitope/details	Within domain IV	Within middle of full length agrin	Within NC1 domain	Within C-terminal G3 domain	Within N-terminal G1 domain	Within G1-IGD-G2 domains	Within G1 domain	-	
Sensitivity to core protein glycosylation	Not sensitive				Increased recognition with deglycosylated core protein				Not sensitive
Enzymatic digestion/other	-			Ch ABC lyase§					-
Antibody dilution	Undiluted supernatant			2.5 μg/mL	4 μg/mL	1 in 20	1 in 30	1 in 25	100 μg/mL
Reference	22			23	24	25	26	27	28

Table 1. Extended

	Biglycan	Lumican	Mimecan	Prolargin	Opticin	Fibromodulin	CD44v3	HAPLN1	HAPLN4
Antibody	AP pAb	AP pAb	329816 mAb	mAb	G21AP	630D1 mAb	3G5 mAb	9/30/8-A-4 mAb	387915 mAb
Source	R&D Systems	R&D Systems	R&D Systems	Abcam	In-house reagent	Enzo Life Sciences	R&D Systems	DSHB	R&D Systems
Epitope/details	-						†	‡	–
Sensitivity to core protein glycosylation	Not sensitive							–	–
Enzymatic digestion/other	-							||	Ch ABC lyase§
Antibody dilution	1 in 10	1 in 20	1 in 20	1 in 25	1 in 100	1 in 50	1 in 100	1 in 50 (concentrate)	1 in 20
Reference	29	30	31	32	33	34	35	36	37

List includes characteristics of antibody epitope on the protein, enzymes applied to tissues prior to antibody treatment, and associated references.

* Developmental Studies Hybridoma Bank (University of Iowa, Iowa City, IA).

† Epitope within the v3 region of CD44.

‡ Two sequestered epitopes within C-terminal half of polypeptide backbone.

§ Chondroitin ABC lyase.

|| Reduction/alkylation, followed by chondroitin AC lyase digestion.

Table 2. Relative Intensity of Fluorescent Staining

	PGs															
	Heparan Sulfate Proteoglycans*			Hyalectans			Short Leucine-Rich Repeat Proteoglycans							Other Proteins		
Tissue Layer	Perlecan	Agrin	Collagen-XVIII	Versican	Aggrecan	Brevican	Decorin	Biglycan	Lumican	Mimecan	Prolargin	Opticin	Fibro-modeulin	CD44v3	HAPLN1	HAPLN4
Internal limiting membrane	+++*	+++	++	+	++	++	+	+	+++	+	++++	++++	+++	+++	+	++
Nerve fiber layer	+	+	+	-	+++	+++	+	+	++	+	+++	++++	+++	+++	+	+++
Ganglion cell layer	+	+	+	-	++	++	+	+	++	+	+++	+++	+++	++	+	+++
Retinal blood vessels	++	+++	++	-	+	+	+	++	+++	+	++	+++	++	++	+	++
Inner plexiform layer	+	+	+	-	++	+++	+	+	++	+	+++	+++	+++	++	+	++
Inner nuclear layer	+	+	+	-	++	++	+	+	++	+	+++	+++	++	++	+	++
Outer plexiform layer	+	+	+	-	++	++	+	+	++	+	+++	++	++	++	+	++
Outer nuclear layer	+	+	+	-	++	++	+	+	++	+	+++	++	++	++	+	++
Interphotoreceptor matrix	+	+	+	-	++	++	+	+	++	+	++	+	++	++	++++	++
Retinal pigment epithelium	++	++	++	+	++	+	+	-	-	-	-	+	+	+	-	+
Bruch's membrane	++	++	++	++	++	+++	++	+++	++++	++	++	++	+++	++	++	++
Choroidal stroma	+	+	+	-	++	++	++	++	+++	++	++	++	++	++	++	+
Choroidal blood vessel walls	++	++	++	++	++	++	++	+++	++++	++	++	++	++	++	++	+
Sclera	++	++	++	+	++++	++	+++	+++	++++	+++	++	++	+++	++	+++	+

Demonstrated using antibodies against proteoglycan core proteins, showing differential staining throughout the tissue layers of the macular region.

* The intensity of staining seen in this study is classified as: –, absent staining; +, weak staining; ++, moderate staining; +++, strong staining; ++++, highly intense staining.

The results were produced from immunohistochemical experiments performed in each case on macular tissue sections from three different adult human eye donors.

Table 3. Proteomic Analysis Showing Number of Unique Peptides and MASCOT Score of Proteoglycan Core Proteins Identified by Tandem Mass Spectrometry for Particular Retinal and Choroidal Tissues

		RPE/Bruch's Membrane/ Choroid		Bruch's Membrane		Neurosensory Retina	
Class of Proteoglycan Core Protein	Proteoglycan Core Protein	Number of Peptides	MASCOT Score*	Number of Peptides	MASCOT Score	Number of Peptides	MASCOT Score
Basement membrane proteoglycans	Perlecan	41	876	46	1403	11	172
	Agrin	6	179	4	72	13	265
	Collagen-XVIII	5	136	0	0	3	70
Hyalectans	Versican	4	137	2	77	0	0
	Aggrecan	1	31	0	0	0	0
Short leucine-rich repeat proteoglycans	Decorin	7	107	6	94	1	56
	Biglycan	12	589	9	383	1	51
	Lumican	19	778	18	848	1	68
	Mimecan	10	393	18	1002	1	74
	Prolargin	4	129	6	185	0	0
	Fibromodulin	0	0	2	51	0	0
Other	CD44	6	155	4	261	4	178
	SPACRCAN	10	442	0	0	8	310

* The MASCOT score signifies the degree of confidence in protein identification, based on the quality of spectral matching. The score for each peptide is calculated as $-10 \times \text{Log}(P)$, where P is the probability that the observed match is a random event.[60] Scores for each peptide have been summed to give the overall score for the protein.

anti-mouse, goat anti-rabbit, goat anti-rat, or rabbit anti-goat; Invitrogen, Paisley, UK), diluted 1:100 in PBS, was added to each tissue section for 2 hours at room temperature. Finally, DAPI was applied as a nuclear counter-stain (at 0.5 μg/mL in PBS for 10 minutes) prior to mounting with medium (Vectashield; Vector Labs, Burlingame, CA) and application of a coverslip. Control experiments were also conducted where tissue sections were treated with blocking buffer instead of primary antibody.

Image Capture and Data Analysis

Images were collected on an upright microscope (Olympus BX51; Olympus, Southend-on-Sea, UK) using a ×10/0.30 Plan Fln objective and captured using a charge-coupled device camera (CoolSNAP ES; Photometrics, Tucson, AZ) operated with bioimaging software (MetaVue v6.1; Molecular Devices, Sunnyvale, CA), as described previously, using specific band pass filter sets for FITC and DAPI.[8,11] Images were analyzed using image processing freeware (ImageJ64 v1.40; provided in the public domain by NIH, Bethesda, MD; http://rsb.info.nih.gov/ij).

Analysis of the staining results from all three donors was performed independently by TDLK and SJC. Both graders were blinded to the experimental conditions, and applied previously agreed scoring criteria to determine the level of staining present in each tissue layer. The scores were averaged to produce Table 2. Where there was background fluorescence (i.e., in the RPE), the graders compared grayscale images of the experiment and the control (i.e., subtracting background autofluorescence) to judge the level of antibody labeling of each core protein.

Results

Proteomic Analysis

The Bruch's membrane, neurosensory retina, and Bruch's/choroid complex samples were subject to anion exchange chromatography in order to enrich any PGs present. Fractions containing PGs were identified with Alcian blue staining (data not shown) and digested with trypsin. Peptides were analyzed by standard liquid chromatography-tandem mass spectrometry methods. PG content was determined in each of the three tissue sample types following successful fragmentation and identification of one or more peptides unique to the relevant PG core protein. The results are summarized below in tabular form separately for each tissue type (see Table 3).

The basement membrane PGs perlecan, agrin and collagen-XVIII were identified in all three tissue samples, with the exception of collagen-XVIII in isolated Bruch's membrane. For the first time to our knowledge, the hyaluronan (HA)-binding proteins (hyalectans), aggrecan and versican were identified in the adult human retina and choroid; versican peptides were found in Bruch's/choroid complex and in Bruch's membrane, while an aggrecan peptide was detected in Bruch's/choroid complex. The SLRPs biglycan, decorin, lumican, and mimecan were identified in all three tissue samples, while fibromodulin and prolargin were found in Bruch's membrane. In addition, CD44 and SPACRCAN were identified in Bruch's membrane/choroid complex and neurosensory retina.

Distribution of Basement Membrane Proteoglycans

Monoclonal antibodies were used to determine further the distribution of perlecan, agrin, and collagen-XVIII in human ocular tissue sections (derived from the macular region) by immunofluorescent microscopy (see Table 1 for details). As illustrated in Figure 1, the antibodies to all three basement membrane PG core proteins labeled the retina, choroid, and sclera; see Table 2 for summary of data derived from the three different donors. Staining of these core proteins was particularly strong in structures containing basement membranes (i.e., at the ILM, the basement membrane of retinal and choroidal blood vessels, and Bruch's membrane). However, there was weaker labeling of other layers of the neurosensory retina and choroidal stroma. The RPE layer appeared to be labeled above background fluorescence with these three antibodies. This was also the case for most of the other antibodies used in this study. However, since the RPE has significant endogenous fluorescence, some caution is needed in drawing firm conclusions regarding the presence of the various PG core proteins in the RPE.

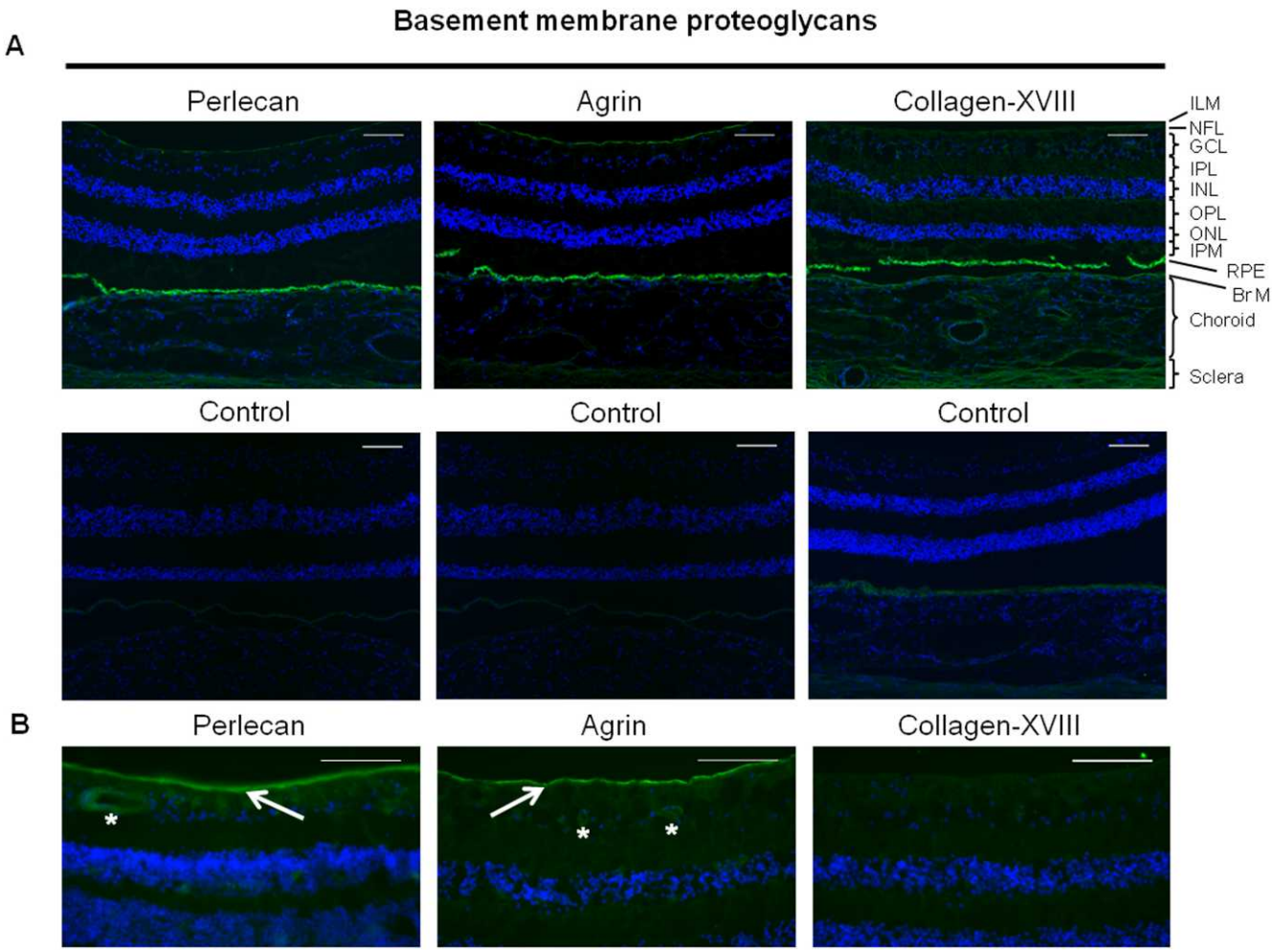

Figure 1. Localization of basement membrane proteoglycans in retina, choroid, and sclera. (**A**) Human ocular tissue sections (macula) were labeled (*green fluorescence*) using antibodies against perlecan, agrin and collagen-XVIII. The accompanying images, shown below, are where the tissue sections were not exposed to the primary antibody. Here, and in all other control experiments (see Supplementary Material and Supplementary Figs. S1–S3, http://www.iovs.org/lookup/suppl/doi:10.1167/iovs.12-10797/-/DCSupplemental), the sections exhibited autofluorescence in the RPE only. In all figures, the images shown are representative of three separate donors, the blue color results from DAPI staining of cell nuclei, and the *white scale bar* indicates 100 μm. In all figures, the following abbreviations are used: ILM, internal limiting membrane; NFL, nerve fiber layer; GCL, ganglion cell layer; IPL, inner photoreceptor layer; INL, inner nuclear layer; OPL, outer photoreceptor layer; ONL, outer nuclear layer; IPM, interphotoreceptor matrix; Br M, Bruch's membrane. (**B**) Higher magnification images of the inner retina are shown in the *lower panels*. The *white arrows* show labeling at the ILM, and the *asterisks* illustrate labeling of blood vessel walls.

Distribution of Hyalectans

Staining for versican (see Fig. 2, Table 2) was seen in Bruch's membrane, surrounding choroidal blood vessels and in the sclera with both the 12C5 and 2B1 antibodies; these monoclonal antibodies were used in conjunction with digestion by chondroitin ABC lyase (see Table 1). These data correlate well with the proteomic analysis, in which versican peptides were identified in the Bruch's/choroid complex and isolated Bruch's membrane, but not in neurosensory retina. However, it is important to note that the proteomic analysis was performed on tissue layers from the whole retina, whereas immunohistochemistry was performed on isolated macular tissue.

The presence of aggrecan was demonstrated throughout the human ocular layers when detected with the monoclonal antibody 179509[25] that was raised against the G1-IGD-G2 domains of aggrecan (see Fig. 2), and a similar staining pattern was seen with the polyclonal antibody B5, which recognizes the G1 domain[26] (data not shown); both antibodies were used after digestion of the sections with chondroitin ABC lyase (see Table 1). In particular, moderate staining was observed throughout the neurosensory retina (strongest in the nerve fiber layer), Bruch's membrane, and choroidal stroma. Labeling of the sclera was extremely strong, which is consistent with a previous study showing the presence of aggrecan in this region.[38]

The distribution of brevican was also analyzed using a monoclonal antibody. Although it was not identified in our proteomic analysis, the distribution of this hyalectan was investigated given its importance in other parts of the central nervous system.[39] Staining for brevican was widespread throughout the retina, Bruch's membrane, choroid, and sclera (Fig. 2).

Distribution of Short Leucine-Rich Repeat Proteoglycan Family Members

Detection of seven different SLRP-family member core proteins (i.e., biglycan, decorin, fibromodulin, lumican, mimecan,

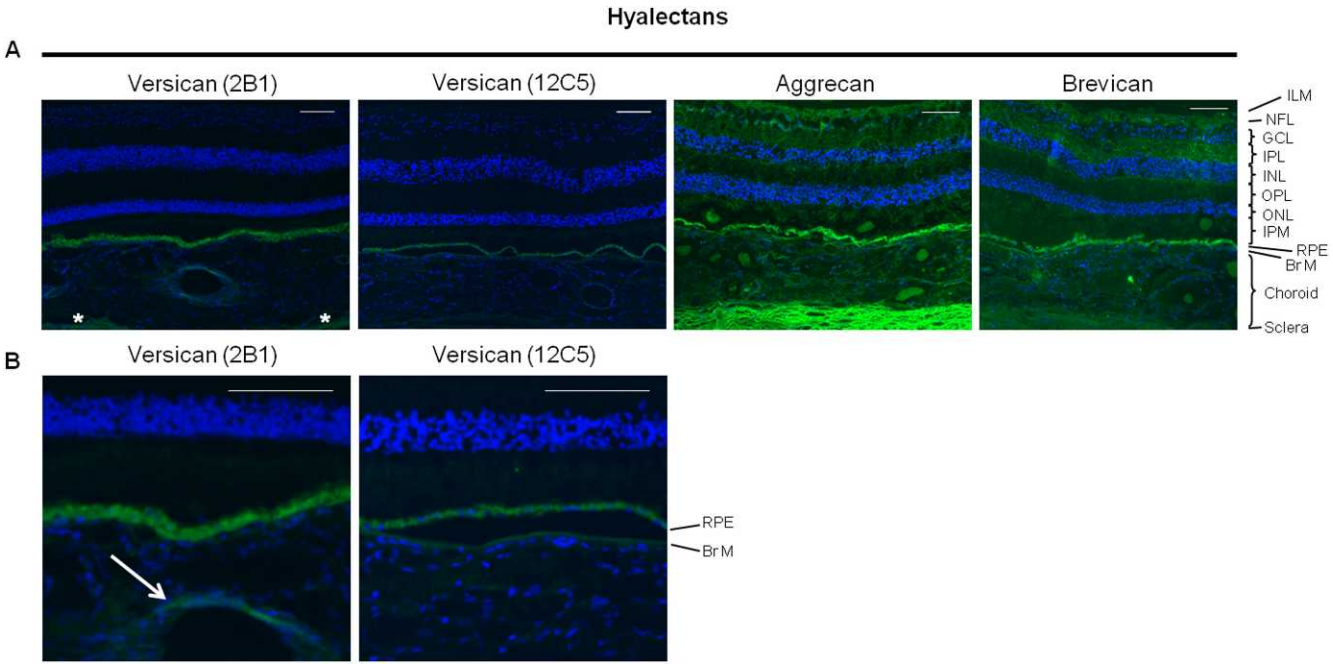

Figure 2. Localization of hyalectans in retina, choroid, and sclera. (**A**) Human ocular tissue sections (macula) were labeled using antibodies against versican, aggrecan, and brevican. In all cases, tissue sections were digested with chondroitin ABC lyase prior to application of antibody (see Table 1). The *asterisks* show labeling of versican in sclera. In all figures, the white scale bar indicates 100 μm. (**B**) Higher magnification images of staining for versican in Bruch's membrane. The *white arrow* shows labeling of versican in choroidal blood vessel walls.

opticin, and prolargin) was carried out using the monoclonal and polyclonal antibodies described in Table 1. Broadly, the staining patterns can be divided into one of two categories (Table 2, Fig. 3).

In the first group, containing biglycan, decorin, lumican, and mimecan, staining was present but weak throughout the layers of the neurosensory retina, and stronger but with varying degrees of staining in Bruch's membrane, choroid, and sclera. In the second group, containing fibromodulin, opticin, and prolargin, staining was much stronger in the neurosensory retina, and was generally moderate throughout Bruch's membrane, choroid, and sclera. In the case of opticin, a gradient of staining was observed whereby the strongest staining was located at the ILM and superficial layers of the neurosensory retina, followed by a gradual decline in staining intensity through the deeper retinal layers towards moderate staining in the choroid. Finally, staining for some PGs revealed labeling of blood cells (e.g., leukocytes and erythrocytes) in the

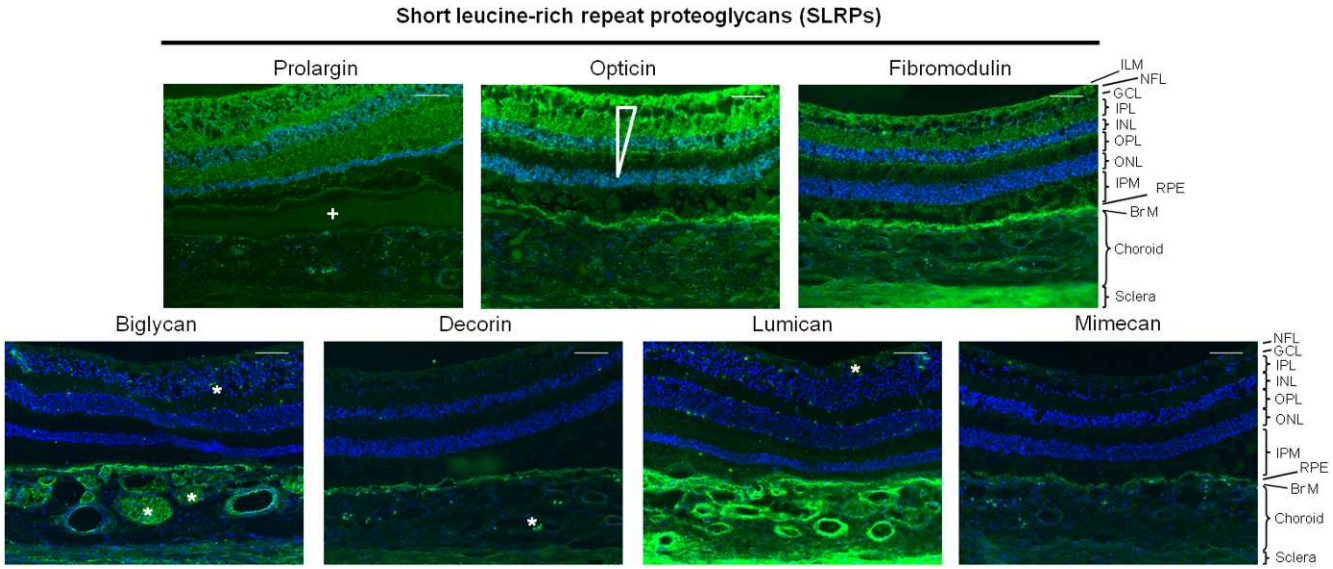

Figure 3. Localization of SLRPs in retina, choroid, and sclera. Human ocular tissue sections (macula) were labeled using antibodies against prolargin, opticin, fibromodulin, biglycan, decorin, lumican, and mimecan. The *white wedge symbol* shows the decreasing gradient of labeling for opticin from the internal limiting membrane through the neurosensory retina toward the choroid. The *asterisks* show the labeling of blood cells (e.g., leukocytes and erythrocytes) in the lumen of choroidal blood vessels and in the neurosensory retina. The *plus sign* illustrates artifactual separation of the neurosensory retina and RPE from Bruch's membrane and choroid. In all figures, the *white scale bar* indicates 100 μm.

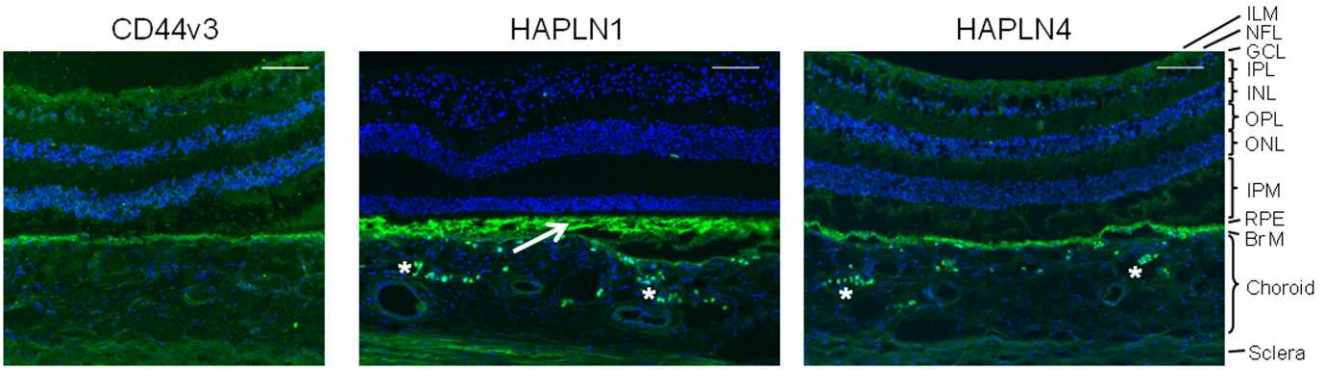

Figure 4. Localization of CD44 and link proteins in retina, choroid, and sclera. Human ocular tissue sections (macula) were labeled using antibodies against CD44v3, HAPLN1 and HAPLN4. The *white arrow* shows very strong labeling of HAPLN1 in the interphotoreceptor matrix, and the *asterisks* show staining (HAPLN1 and HAPLN4) of leukocytes in the choroid. In all figures, the *white scale bar* indicates 100 μm.

lumen of choroidal blood vessels (e.g., for biglycan and decorin) and/or in the neurosensory retina (e.g., for biglycan and lumican).

Distribution of Other Proteins

The staining pattern for CD44v3 was analyzed in this study using a monoclonal antibody. This was undertaken because CD44 peptides were found in our proteomic analysis (Table 3), and CD44v3 (a CD44 isoform arising from variable exon splicing) can exist as an HS PG.[40] Staining for CD44v3 was present at moderate levels throughout all layers of the retina, choroid, and sclera, though with somewhat stronger staining at the ILM and nerve fiber layer (Fig. 4).

The distribution of two link proteins (HAPLNs) was analyzed, given that we identified aggrecan and versican in the human retina (Fig. 2) and previously identified HA throughout the human retina and choroid,[11] and since link proteins stabilize the interactions between hyalectans and HA.[37] HAPLN1 (cartilage link protein) and HAPLN4 (brain link protein 2) were detected with monoclonal antibodies following pretreatment of the tissue sections (see Table 1). This is the first time to our knowledge that these link proteins have been observed in the human retina. Staining for HAPLN1 was particularly strong in the IPM and sclera, while staining for HAPLN4 was moderate throughout the neurosensory retina and Bruch's membrane, but with stronger labeling of the nerve fiber and ganglion cell layers. In both cases, labeling of blood cells (presumably leukocytes) was observed in the lumen of choroidal blood vessels.

Discussion

In this study, we have used proteomic analysis to identify PG core proteins in the posterior segment of human eye tissue and demonstrated the presence of basement membrane PGs, hyalectans and PGs from the SLRP family. This was combined with immunofluorescence microscopy and showed that the different PG core proteins have distinctive distributions throughout the layers of the macular retina, choroid, and sclera. We extracted and partially purified PGs by ion-exchange chromatography prior to proteomic analysis. However, since the PG core proteins could have had other charged modifications such as sialylated oligosaccharides, which allowed them to bind to the ion-exchange column, we cannot assume that they were all GAG-modified. Furthermore, the PG core proteins identified by immunofluorescence could potentially have been GAG-modified, oligosaccharide-modified, or non-glycosylated core proteins.

Because both the proteomics and the immunohistochemistry methodologies employed are qualitative techniques, we do not make any inferences regarding the relative or absolute amounts of the PG core proteins in the tissues. Also, the list of PG core proteins identified by mass spectrometry is not exhaustive since peptide absence does not necessarily imply that a particular protein was absent from the sample.[41] There could be a number of reasons for this, including the fact that we did not deglycosylate the samples prior to trypsin digestion, and only a subset of chromatography fractions was selected for analysis. However, a previously published proteomic study, which did not enrich for PGs by ion-exchange chromatography, identified a very similar list of PG core proteins (i.e., perlecan, agrin, collagen-XVIII, glypican-6, decorin, biglycan, lumican, prolargin, mimecan, fibromodulin, and CD44) in human RPE/Bruch's membrane/choroid tissue.[42] Whilst we did not identify glypican-6 in the Bruch's/choroid complex, we did additionally identify the hyalectans versican and aggrecan, and this is the first report to our knowledge of their presence in the human retina.

With regard to the basement membrane PG core proteins, our findings are consistent with previous immunohistochemical studies of perlecan,[16,19] agrin,[19] and collagen-XVIII.[18] Our findings are also consistent with those of Halfter and colleagues who used the same antibodies against perlecan, agrin, and collagen-XVIII to study the ILM.[17] However, unlike the previous studies, we analyzed the distribution of these PG core proteins through the whole thickness of the macular retina and choroid, and performed this alongside a comprehensive analysis of the other PG core proteins in the same tissues. This approach has revealed highly distinct patterns of localization, both between classes of PG core proteins (e.g., basement membrane PGs versus SLRPs) and between members of individual classes (e.g., lumican versus prolargin).

The distribution of the basement membrane PGs may have important implications in the human eye. A mutation in the gene for collagen-XVIII associated with Knobloch syndrome in humans suggests that this PG plays a critical role in the development of retinal vasculature and maintenance of retinal structure.[43] Peptides derived by proteolysis of the C-terminus of collagen-XVIII (endostatin) and perlecan (endorepellin) have anti-angiogenic activity,[44] and may inhibit preretinal and choroidal neovascularization. In this context, it is of interest that our proteomic analysis demonstrated that perlecan peptides are particularly abundant in Bruch's membrane.

To our knowledge, the hyalectans versican, aggrecan and brevican have not previously been reported in the human retina or choroid. Versican has been identified in the human vitreous.[45] It has also been detected by immunohistochemistry in the nerve fiber and inner plexiform layers of the embryonic chick retina.[14] However, versican immunoreactivity decreased in the adult chick retina, leaving staining only in the photoreceptor layer and Bruch's membrane, which resembles somewhat our findings in the human (i.e., staining in Bruch's membrane and choroidal blood vessels). Versican and aggrecan have been detected in the rat retina.[13] In the embryonic rat, immunoreactivity for versican and aggrecan was observed in the inner retinal layers. In the adult rat, immunoreactivity for both was strong in the ganglion cell and plexiform layers and weak in the nuclear layers and choroid. Hence, our findings for human macular tissue are generally similar in the case of aggrecan, but quite different in the case of versican. More recently, aggrecan has been detected throughout the mouse retina.[12] In the adult mouse, immunoreactivity was strong in the ganglion cell and nuclear layers and weak in the inner plexiform and photoreceptor layers. Hence, it is apparent that substantial species-specific differences exist for these PG core proteins. We are not aware of any reports of the presence of brevican in perinatal or adult retinal tissues of any vertebrate animals.

These findings, together with the clinical phenotype of Wagner syndrome, suggest that the hyalectans may have important roles in the development and maintenance of the human retina. Wagner syndrome is characterized clinically by vitreous abnormalities and chorioretinal atrophy, often followed by retinal detachment, and is caused by mutations that alter splicing of the versican gene (*CSPG2*).[46] Whereas versican was known to be present in human vitreous, our novel finding of its localization to Bruch's membrane may suggest new mechanisms to explain some clinical features of Wagner syndrome (e.g., chorioretinal atrophy).

The ocular distribution of the SRLP core proteins has been studied in some animal species. For example, decorin was detected throughout the neurosensory retina of the mouse[12] and rat.[47] Its importance in retinal development has been demonstrated in a recent study of the avian embryo, where inhibition of decorin function led to loss of polarization in retinal progenitor cells, along with many other abnormalities.[48] Interestingly, our study demonstrates more abundant labeling of decorin in Bruch's membrane and choroid than the neurosensory retina, though it is possible that decorin expression is different in embryological stages.

Biglycan distribution has been examined in the mouse eye, where it was located throughout the retina in both embryological and adult stages.[12] By comparison, our data do demonstrate the presence of biglycan in the neurosensory retina, but labeling of this core protein was much more abundant in Bruch's membrane and the choroid. Importantly, mice overexpressing biglycan show a marked increase in Bruch's membrane thickness, with potential implications for theories of AMD pathogenesis.[49] In general, biglycan and decorin are both thought to act as neurotrophic factors for retinal cells, and as regulators of their differentiation,[12] and our study has revealed they share a similar distribution throughout the layers of the human macular retina and choroid.

Lumican is an important SLRP of the sclera and cornea,[50,51] but there have been no immunohistochemical reports of its presence in the retina or choroid. This SLRP is involved in the regulation of collagen fibrillogenesis, including fibril diameter and interfibrillar spacings, and may also have proinflammatory effects.[52] Interestingly, polymorphisms in the lumican gene have been linked to high myopia in humans,[53] and lumican-fibromodulin double-null mice exhibit increased axial length and frequent retinal detachments.[54] Our findings confirmed the presence of lumican in human sclera, but also demonstrated abundant core protein in Bruch's membrane, choroid and (to a lesser extent) neurosensory retina including the IPM. These novel findings warrant further investigation; its localization to these layers may suggest new mechanisms to explain high myopia and retinal detachment (e.g., lumican in the IPM could be involved). In addition, it is possible that lumican is required for the pentalaminar structural integrity of Bruch's membrane (e.g., through regulation of collagen fibril spacing in the collagenous layers).

Similarly, mimecan is known to be present in the sclera and cornea, but its novel immunolocalization in the human retina and choroid requires further study. In addition, our previous finding that KS is absent from the human retina and choroid[11] suggests that, unlike in the cornea, lumican and mimecan core proteins are not modified with KS chains in these locations, with similar conclusions for prolargin and fibromodulin. Prolargin, for example, is known to be substituted with KS GAG in both the human sclera and cornea,[50] but has never been studied in the retina or choroid.

We have examined the distribution of opticin previously in the human eye, where it was localized mainly in the vitreous humor and ILM.[55] However, for the current study, we used the more sensitive method of immunofluorescence microscopy and detected a more widespread distribution. Opticin is thought to be secreted by the ciliary body into the vitreous cavity,[56] so our finding of a gradient distribution from the ILM to the choroid support the idea that opticin may diffuse from the vitreous through the neurosensory retina to be carried away in the choroid. Interestingly, opticin has antiangiogenic properties,[33,57] so its abundance in the ILM and superficial retinal layers may help prevent pathological proliferative retinopathies (i.e., by inhibiting the growth of blood vessels from the retina into the vitreous).

The distribution of link proteins was analyzed because we identified aggrecan and versican as well as HA in the human retina,[11] and link proteins stabilize the interactions between HA and these hyalectans.[37] This is the first report to our knowledge that discusses the presence of HAPLN1 and HAPLN4 in the human retina, though HAPLN1 has been reported at this location in chick embryos.[58] Our data show that HAPLN1 is highly abundant in the IPM, where there is also staining for aggrecan and HA, and it is possible that complexes between PGs, HA, and HAPLN1 (that give structural integrity in other tissues—e.g., brain and blood vessel walls) may contribute to retinal attachment at this location. By contrast, HAPLN4 (or brain link protein 2) was found throughout the neurosensory retina, with strong labeling of the nerve fiber and ganglion cell layers. In the brain, aggrecan is a component of perineuronal nets, important extracellular matrix structures involved in synaptic stabilization, and reduced plasticity.[59] It is possible that perineuronal nets in the neurosensory retina are formed by complexes between aggrecan, HA and HAPLN4, and our findings warrant further investigation, particularly given recent interest in using chondroitin ABC lyase to reverse glaucoma by disrupting perineuronal nets (Morgan J, et al. *IOVS* 2010:ARVO E-Abstract 2517).

In conclusion, this study provides a comprehensive analysis of PG core protein localization throughout the human retina, choroid, and sclera. This demonstrates that different core protein families and family members have very distinct distribution patterns in macular tissue. In combination with our recent study of GAG chains, this will greatly assist further research into the regulation of ocular tissue in development, health and disease.

Acknowledgments

The authors thank Isaac Zambrano (Manchester Eye Bank, Manchester Royal Eye Hospital, Manchester, UK) for supplying the donor eye tissue used in this study. We also thank Timothy Hardingham (University of Manchester, UK) and Thomas Wight (Benaroya Research Institute at Virginia Mason, Seattle) for their donation of antibodies used in this study. The monoclonal antibodies 5C9, 6D2, 6C4 (developed by William Halfter) and 8A4 (developed by Bruce Caterson) were obtained from the Developmental Studies Hybridoma Bank developed under the auspices of the NICHD and maintained by The University of Iowa, Department of Biology, Iowa City, IA 52242.

References

1. Sarrazin S, Lamanna WC, Esko JD. Heparan sulfate proteoglycans. *Cold Spring Harb Perspect Biol*. 2011;3:pii:a004952.
2. Iozzo RV, Schaefer L. Proteoglycans in health and disease: novel regulatory signaling mechanisms evoked by the small leucine-rich proteoglycans. *FEBS J*. 2010;277:3864–3875.
3. Inatani M, Tanihara H. Proteoglycans in retina. *Prog Ret Eye Res*. 2002;21:429–447.
4. Schaefer L, Schaefer RM. Proteoglycans: from structural compounds to signaling molecules. *Cell Tissue Res*. 2010; 339:237–246.
5. Ichijo H. Proteoglycans as cues for axonal guidance in formation of retinoctectal or retinocollicular projections. *Mol Neurobiol*. 2004;30:23–33.
6. Lazarus HS, Hageman GS. Xyloside-induced disruption of interphotoreceptor matrix proteoglycans results in retinal detachment. *Invest Ophthalmol Vis Sci*. 1992;33:364–376.
7. Booij JC, Baas DC, Beisekeeva J, et al. The dynamic nature of Bruch's membrane. *Prog Ret Eye Res*. 2010;29:1–18.
8. Clark SJ, Perveen R, Hakobyan S, et al. Impaired binding of the age-related macular degeneration-associated complement factor H 402H allotype to Bruch's membrane in human retina. *J Biol Chem*. 2010;285:30192–30202.
9. Clark SJ, Bishop PN, Day AJ. Complement factor H and age-related macular degeneration: the role of glycosaminoglycan recognition in disease pathology. *Biochem Soc Trans*. 2010;38: 1342–1348.
10. Day AJ, Clark SJ, Bishop PN. Understanding the molecular basis of age-related macular degeneration and how the identification of new mechanisms may aid the development of novel therapies. *Expert Rev Ophthalmol*. 2011;6:123–128.
11. Clark SJ, Keenan TDL, Fielder H, et al. Mapping the differential distribution of glycosaminoglycans in the adult human retina, choroid and sclera. *Invest Ophthalmol Vis Sci*. 2011;52:6511–6521.
12. Ali SA, Hosaka YZ, Uehara M. Spatiotemporal distribution of chondroitin sulfate proteoglycans in the developing mouse retina and optic nerve. *J Vet Med Sci*. 2011;73:13–18.
13. Popp S, Maurel P, Andersen JS, Margolis RU. Developmental changes of aggrecan, versican and neurocan in the retina and optic nerve. *Exp Eye Res*. 2004;79:351–356.
14. Zako M, Shinomura T, Miyaishi O, et al. Transient expression of PG-M/versican, a large chondroitin sulfate proteoglycan in developing chicken retina. *J Neurochem*. 1997;69:2155–2161.
15. McAdams BD, McLoon SC. Expression of chondroitin sulfate and keratan sulfate proteoglycans in the path of growing retinal axons in the developing chick. *J Comp Neurol*. 1995; 352:594–606.
16. Johnson PT, Betts KE, Radeke MJ, et al. Individuals homozygous for the age-related macular degeneration risk-conferring variant of complement factor H have elevated levels of CRP in the choroid. *Proc Natl Acad Sci U S A*. 2006;103:17456–17461.
17. Halfter W, Dong S, Schurer B, et al. Embryonic synthesis of the inner limiting membrane and vitreous body. *Invest Ophthalmol Vis Sci*. 2005;46:2202–2209.
18. Bhutto IA, Kim SY, McLeod DS, et al. Localization of collagen XVIII and the endostatin portion of collagen XVIII in aged human control eyes and eyes with age-related macular degeneration. *Invest Ophthalmol Vis Sci*. 2004;45:1544–1552.
19. Witmer AN, van den Born J, Vrensen GFJM, Schlingemann RO. Vascular localization of heparan sulfate proteoglycans in retinas of patients with diabetes mellitus and in VEGF-induced retinopathy using domain-specific antibodies. *Curr Eye Res*. 2001;22:190–197.
20. Wall RS, Gyi TJ. Alcian blue staining of proteoglycans in polyacrylamide gels using the critical electrolyte concentration approach. *Analytical Biochem*. 1988;175:298–299.
21. Pierce A, Williamson A, Jaworska E, et al. Identification of nuclear protein targets for six leukemogenic tyrosine kinases governed by post-translational regulation. *PLoS One*. 2012;7: e38928.
22. Halfter W. A heparan sulfate proteoglycan in developing avian axonal tracts. *J Neurosci*. 1993;13:2863–2873.
23. Isogai Z, Shinomura T, Yamakawa N, et al. 2B1 antigen characteristically expressed on extracellular matrices of human malignant tumors is a large chondroitin sulfate proteoglycan, PG-M/versican. *Cancer Res*. 1996;56:3902–3908.
24. Asher RA, Mergenstern DA, Shearer MC, et al. Versican is upregulated in CNS injury and is a product of oligodendrocyte lineage cells. *J Neurosci*. 2002;22:2225–2236.
25. Virgintino D, Perissinotto D, Girolamo F, et al. Differential distribution of aggrecan isoforms in perineuronal nets of the human cerebral cortex. *J Cell Mol Med*. 2009;13:3151–3173.
26. Dudhia J, Davidson CM, Wells TM, et al. Age-related changes in the content of the C-terminal region of aggrecan in human articular cartilage. *Biochem J*. 1996;313:933–940.
27. R&D Systems, Inc. Monoclonal anti-human brevican antibody. Available at: http://www.rndsystems.com/pdf/MAB40091.pdf. Accessed July 12, 2012.
28. Brézillon S, Venteo L, Ramont L, et al. Expression of lumican, a small leucine-rich proteoglycan with antitumour activity, in human malignant melanoma. *Clin Exp Dermatol*. 2007;32: 405–416.
29. Kitaya K, Yasuo T. Dermatan sulfate proteoglycan biglycan as a potential selectin L/CD44 ligand involved in selective recruitment of peripheral blood CD16(-) natural killer cells into human endometrium. *J Leukoc Biol*. 2009;85:391–400.
30. Zhang Y, Conrad AH, Conrad GW. Effects of ultraviolet-A and riboflavin on the interaction of collagen and proteoglycans during corneal cross-linking. *J Biol Chem*. 2011;286:13011–13022.
31. R&D Systems, Inc. Human mimecan antibody. Available at: http://www.rndsystems.com/pdf/MAB2660.pdf. Accessed July 12, 2012.
32. Abcam, Inc. Anti-PRELP antibody. Available at: http://www.abcam.com/PRELP-antibody-ab76511.pdf. Accessed July 12, 2012.
33. Goff MM, Lu H, Ugarte M, et al. The vitreous glycoprotein opticin inhibits preretinal neovascularisation. *Invest Ophthalmol Vis Sci*. 2012;53:228–234.
34. Adamczyk C, Milz S, Tischer T, Putz R, Benjamin M. An immunohistochemical study of the extracellular matrix of entheses associated with the human pisiform bone. *J Anat*. 2008;212:645–653.
35. Rosenberg WM, Prince C, Kaklamanis L, et al. Increased expression of CD44v6 and CD44v3 in ulcerative colitis but not colonic Crohn's disease. *Lancet*. 1995;345:1205–1209.

36. Milz S, Regner F, Putz R, Benjamin M. Expression of a wide range of extracellular matrix molecules in the tendon and trochlea of the human superior oblique muscle. *Invest Ophthalmol Vis Sci*. 2002;43:1330–1334.
37. Binette F, Cravens J, Kahoussi B, Haudenschild DR, Goetinck PF. Link protein is ubiquitously expressed in non-cartilaginous tissues where it enhances and stabilizes the interaction of proteoglycans with hyaluronic acid. *J Biol Chem*. 1994;269: 19116–19122.
38. Rada JA, Achen VR, Perry CA, Fox PW. Proteoglycans in the human sclera. Evidence for the presence of aggrecan. *Invest Ophthalmol Vis Sci*. 1997;38:1740–1751.
39. Theocharis AD, Skandalis, SS, Tzanakakis GN, Karamanos NK. Proteoglycans in health and disease: novel roles for proteoglycans in malignancy and their pharmacological targeting. *FEBS J*. 2010;277:3904–3923.
40. Jackson DG, Bell JI, Dickinson R, Timans J, Shields J, Whittle N. Proteoglycan forms of the lymphocyte homing receptor CD44 are alternatively spliced variants containing the v3 exon. *J Cell Biol*. 1995;128:673–685.
41. Roepstorff P. Mass spectrometry based proteomics, background, status and future needs. *Protein Cell*. 2012;3:641–647.
42. Yuan X, Gu X, Crabb JS, et al. Quantitative proteomics: comparison of the macular Bruch membrane/choroid complex from age-related macular degeneration and normal eyes. *Mol Cell Proteomics*. 2010;9:1031–1046.
43. Sertie AL, Sossi V, Camargo AA, et al. Collagen XVIII, containing an endogenous inhibitor of angiogenesis and tumor growth, plays a critical role in the maintenance of retinal structure and in neural tube closure (Knobloch syndrome). *Hum Mol Genet*. 2000;9:2051–2058.
44. Goyal A, Pal N, Concannon M, et al. Endorepellin, the angiostatic module of perlecan, interacts with both the $\alpha 2\beta 1$ integrin and vascular endothelial growth factor receptor 2 (VEGFR2): a dual receptor antagonism. *J Biol Chem*. 2011; 286:25947–25962.
45. Reardon A, Heinegård D, McLeod D, Sheehan JK, Bishop PN. The large chondroitin sulphate proteoglycan versican in mammalian vitreous. *Matrix Biol*. 1998;17:325–333.
46. Meredith SP, Richards AJ, Flanagan DW, Scott JD, Poulson AV, Snead MP. Clinical characterisation and molecular analysis of Wagner syndrome. *Br J Ophthalmol*. 2007;91:655–659.
47. Inatani M, Tanihara H, Honjo M, Hangai M, Kresse H, Honda Y. Expression of proteoglycan decorin in neural retina. *Invest Ophthalmol Vis Sci*. 1999;40:1783–1791.
48. Zagris N, Gilipathi K, Soulintzi N, Konstantopoulos K. Decorin developmental expression and function in the early avian embryo. *Int J Dev Biol*. 2011;55:633–639.
49. Sallo FB, Bereczki E, Csont T, et al. Bruch's membrane changes in transgenic mice overexpressing the human biglycan and apolipoprotein b-100 genes. *Exp Eye Res*. 2009;89:178–186.
50. Johnson JM, Young TL, Rada JA. Small leucine rich repeat proteoglycans (SLRPs) in the human sclera: identification of abundant levels of PRELP. *Mol Vis*. 2006;12:1057–1066.
51. Chakravarti S, Petroll WM, Hassell JR, et al. Corneal opacity in lumican-null mice: defects in collagen fibril structure and packing in the posterior stroma. *Invest Ophthalmol Vis Sci*. 2000;41:3365–3373.
52. Ying S, Shiraishi A, Kao CW, et al. Characterization and expression of the mouse lumican gene. *J Biol Chem*. 1997; 272:30306–30313.
53. Lin HJ, Kung YJ, Lin YJ, et al. Association of the lumican gene functional 3′-UTR polymorphism with high myopia. *Invest Ophthalmol Vis Sci*. 2010;51:96–102.
54. Chakravarti S, Paul J, Roberts L, Chervoneva I, Oldberg A, Birk DE. Ocular and scleral alterations in gene-targeted lumican-fibromodulin double-null mice. *Invest Ophthalmol Vis Sci*. 2003;44:2422–2432.
55. Ramesh S, Bonshek RE, Bishop PN. Immunolocalisation of opticin in the human eye. *Br J Ophthalmol*. 2004;88:697–702.
56. Bishop PN, Takanosu M, Le Goff M, et al. The role of the posterior ciliary body in the biosynthesis of vitreous humour. *Eye*. 2002;16:454–460.
57. Le Goff MM, Sutton MJ, Slevin M, Latif A, Humphries MJ, Bishop PN. Opticin exerts its anti-angiogenic activity by regulating extracellular matrix adhesiveness. *J Biol Chem*. 2012;287:28027–28036.
58. Tsonis PA, Goetinck PF. Expression of cartilage-matrix genes and localization of their translation products in the embryonic chick eye. *Exp Eye Res*. 1988;46:753–764.
59. Carulli D, Pizzorusso T, Kwok JC, et al. Animals lacking link protein have attenuated perineuronal nets and persistent plasticity. *Brain*. 2010;133:2331–2347.
60. Matrix Science, Inc. Matrix Science. Available at: http://www.matrixscience.com. Accessed July 12, 2012.